Zitierweise: *Angew. Chem. Int. Ed.* **2025**, *64*, e202517004
doi.org/10.1002/anie.202517004

Halogen Bonds

Mechanochemical *Cis/Trans* Isomerization of a Metal Centre Involving a Metal-Organic Halogen-Bonded (MOXB) Cocrystal

Katarina Lisac, Luzia S. Germann, Mihails Arhangelskis, Martin Etter, Robert E. Dinnebier, Tomislav Friščić, and Dominik Cinčić**

Abstract: Halogen bonding enables the mechanochemical ball-milling isomerization of an otherwise persistent *cis*-coordinated metal complex into the corresponding *trans*-isomer. The importance of halogen bonding for enabling the *cis*→*trans* isomerization of the metal centre is evidenced by real-time in situ synchrotron powder X-ray diffraction monitoring of the ball-milling experiments that showed the transient appearance of a *cis*-geometry metal-organic halogen-bonded (MOXB) cocrystal, which is rapidly replaced by the corresponding *trans*-geometry one, with any excess, non-halogen-bonded *cis*-geometry complex being retained throughout the milling experiment. The importance of cocrystallization for *cis*→*trans* isomerization is supported by periodic density-functional theory calculations which show that the process becomes notably more enthalpically favourable in the presence of the halogen bond donor. The presented work indicates that the formation of MOXB cocrystals can open the door to new, metal-based responsive behaviours, different from those of parent solid-state coordination complexes.

Cocrystallization represents an important supramolecular solid-state strategy in developing solids with improved or new properties, particularly in the contexts of pharmaceutical solids,[1–3] agrochemicals,[4–6] optical materials,[7,8] organic semiconductors,[9] and energetic materials.[10–12] The halogen bond has emerged as a highly versatile directional interaction with applications for crystal engineering of multicomponent solids, notably cocrystals.[13,14] While the majority of studies on halogen-bonded cocrystals have focused on organic molecular systems,[13–17] much less attention has been dedicated to metal-organic ones. Metal-organic halogen-bonded (MOXB) cocrystals are of interest[18–21] due to the opportunity to introduce metal-related electrical, magnetic, catalytic, optical and other properties to the self-assembled materials.[22–24] Furthermore, metal complexes provide geometries not usually accessible to organic molecules (e.g., square-planar, trigonal-bipyramidal, square pyramidal, or octahedral) which makes them desirable as building blocks for new crystal structures. Finally, many metal complexes can form different types of isomers, structural and stereo-isomers, which expands possibilities for preparing different crystal phases with desirable properties.[15] Our group has previously demonstrated a general strategy for the design and synthesis of MOXB cocrystals based on coordination complexes that can engage in halogen bonding via chloride ions coordinated to the metal centre as acceptors.[25–28]

Here we report how the formation of a MOXB cocrystal enables mechanochemical *cis*→*trans* isomerization of an octahedral *cis*-coordinated cobalt(II) complex, which does not undergo such an isomerization on its own. Specifically, whereas solution synthesis selectively provides the crystalline *cis*-geometry metal complex, which does not undergo isomerization upon mechanical treatment on its own, ball-milling in the presence of the halogen bond donor 1,4-diiodotetraflurobenzene (**14tfib**) leads to cocrystallization and subsequent conversion into the corresponding *trans*-coordinated complex. That the *cis*-complex on its own does not undergo isomerization and that the mechanochemical *cis*→*trans* isomerization is mediated by the formation of

[*] Dr. K. Lisac, Prof. Dr. D. Cinčić
Department of Chemistry, Faculty of Science, University of Zagreb, Horvatovac 102a, Zagreb 10000, Croatia
E-mail: dominik@chem.pmf.hr

Dr. K. Lisac
Ruđer Bošković Institute, Bijenička Cesta 54, Zagreb 10000, Croatia

Dr. L. S. Germann, Prof. Dr. R. E. Dinnebier
Max Planck Institute for Solid State Research, Stuttgart 70569, Germany

Dr. L. S. Germann, Prof. Dr. T. Friščić
Department of Chemistry, McGill University, Montreal H3A 0B8, Canada
E-mail: t.friscic@bham.ac.uk

Associate Prof. Dr. M. Arhangelskis
Faculty of Chemistry, University of Warsaw, Warsaw 02–093, Poland

Dr. M. Etter
Deutsches Elektronen-Synchrotron (DESY), Hamburg 22607, Germany

Prof. Dr. T. Friščić
School of Chemistry, University of Birmingham, Edgbaston, Birmingham B15 2TT, UK

Additional supporting information can be found online in the Supporting Information section

a MOXB cocrystal is evidenced by real-time in situ synchrotron powder X-ray diffraction (PXRD) monitoring of milling experiments, as well as by laboratory *ex situ* studies. While previous studies have shown how cocrystallization can stabilize or direct the synthesis of certain isomers of organic molecules,[29,30] the current work is to the best of our knowledge the first to demonstrate halogen bond-based cocrystallization as a means to impart isomerization behaviour to an otherwise inert coordination complex in the solid state.

The focus of this study is the complex *bis*(2-benzoylpyridine)dichloridocobalt(II) ($CoCl_2$**bzpy**$_2$) (Figure 1), obtained as a crystalline solid by solution-phase reaction of $CoCl_2{\cdot}6H_2O$ and the ligand **bzpy** exclusively in the *cis*-form (*cis*-$CoCl_2$**bzpy**$_2$), as evidenced by single crystal X-ray diffraction analysis (see Supporting Information). In contrast, solution synthesis in the presence of **14tfib** was found to lead to three distinct MOXB cocrystals, of compositions (*cis*-$CoCl_2$**bzpy**$_2$)(**14tfib**)$_2$, (*cis*-$CoCl_2$**bzpy**$_2$)(**14tfib**), and (*trans*-$CoCl_2$**bzpy**$_2$)(**14tfib**)$_2$, sometimes in a mixture, that were all characterized by single crystal X-ray diffraction (see Supporting Information). The appearance of the (*trans*-$CoCl_2$**bzpy**$_2$)(**14tfib**)$_2$ phase is surprising, considering that solution-based synthesis and crystallization of *cis*-$CoCl_2$**bzpy**$_2$ alone did not lead to the *trans*-isomer, indicating a role of the XB donor in enabling the *cis*→*trans* isomerization. The crystal structures in all cases reveal one-dimensional (1D) chains of C─I···Cl─Co halogen bonds involving **14tfib** as the XB donor, with the chloride ligands of the *cis*- or the *trans*-metal-organic building block acting as the acceptor (Figure 1). In the MOXB cocrystals (*cis*-$CoCl_2$**bzpy**$_2$)(**14tfib**)$_2$ and (*trans*-$CoCl_2$**bzpy**$_2$)(**14tfib**)$_2$, in which the respective ratio of XB acceptors and donors is 1:2, the 1D chains are further modified by additional **14tfib** molecules: in (*cis*-$CoCl_2$**bzpy**$_2$)(**14tfib**)$_2$ the 1D chains are decorated by **14tfib** molecules through I···I halogen bonds, while in (*trans*-$CoCl_2$**bzpy**$_2$)(**14tfib**)$_2$ the additional **14tfib** molecules cross-link the 1D chains through I···Cl halogen bonds to form two-dimensional (2D) sheets of square-grid layer (*sql*) topology. The relative thermodynamic stabilities of all cocrystals and reactions leading to their formation were calculated through periodic density-functional theory (DFT) calculations.[31–33]

Next, cocrystal synthesis was attempted mechanochemically, by either ball-milling in the presence of a liquid additive (liquid-assisted grinding, LAG)[34–38] or by manual grinding with a liquid additive (kneading),[39,40] methodologies that both use a small amount of a liquid phase to facilitate transformations (Scheme 1). Kneading reactions were performed by using an agate mortar (60 mm in diameter) and a pestle (18 mm in diameter and 70 mm in length), while LAG reactions were conducted with reaction mixtures placed in stainless steel jars, and shaken at a frequency of 25 Hz using a Retsch MM200 mill using two stainless steel balls of 5 mm diameter (0.5 gram weight each). In all cases, ethanol (EtOH) was used as a liquid additive. The laboratory air temperature during experiments was ca. 25 °C, and relative humidity (RH) varied from 40%–50% (see Supporting Information). The

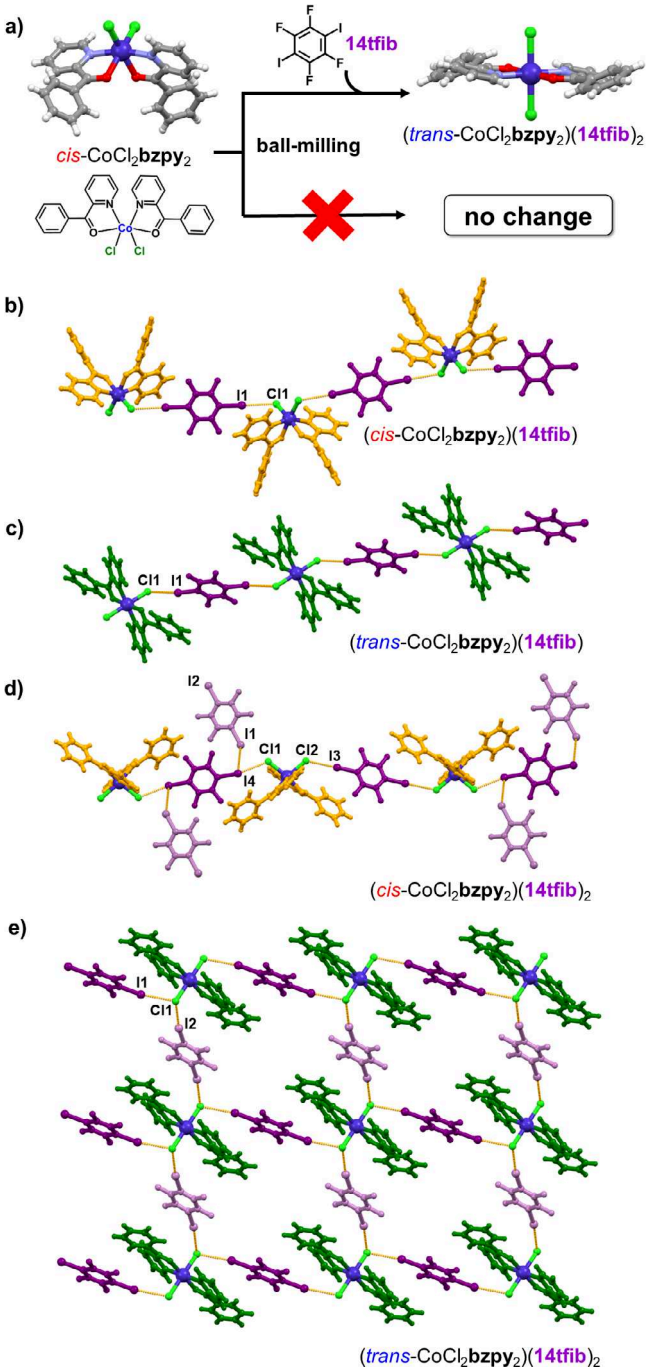

Figure 1. a) The cocrystallization-enabled *cis*→*trans* isomerization of the complex $CoCl_2$**bzpy**$_2$, with the chemical diagram and molecular structures of both isomers shown, as found in pure solid *cis*-$CoCl_2$**bzpy**$_2$ and a **14tfib** cocrystal of *trans*-$CoCl_2$**bzpy**$_2$. Crystal structures of cocrystals: b) (*cis*-$CoCl_2$**bzpy**$_2$)(**14tfib**), c) (*trans*-$CoCl_2$**bzpy**$_2$)(**14tfib**), d) (*cis*-$CoCl_2$**bzpy**$_2$)(**14tfib**)$_2$, and e) (*trans*-$CoCl_2$**bzpy**$_2$)(**14tfib**)$_2$.The I···Cl halogen bonds are shown as yellow dashed lines. Halogen bonds parameters for b) (*cis*-$CoCl_2$**bzpy**$_2$)(**14tfib**): $d_{I\cdots Cl}$ = 3.178(1) Å, $\angle_{C-I\cdots Cl}$ = 177.89(8)°; c) (*trans*-$CoCl_2$**bzpy**$_2$)(**14tfib**): $d_{I\cdots Cl}$ = 3.138(5) Å, $\angle_{C-I\cdots Cl}$ = 172.0(2)°; d) (*cis*-$CoCl_2$**bzpy**$_2$)(**14tfib**)$_2$: $d_{I3\cdots Cl1}$ = 3.189(1) Å, $d_{I4\cdots Cl2}$ = 3.197(1) Å; $\angle_{C-I\cdots Cl}$ = 178.9(2)°, $\angle_{C-I\cdots Cl}$ = 167.3(2)°, $d_{I1\cdots I4}$ = 3.9512(8) Å, $\angle_{C-I\cdots I}$ = 140.29°; e) (*trans*-$CoCl_2$**bzpy**$_2$)(**14tfib**)$_2$: $d_{I1\cdots Cl1}$ = 3.197(2) Å, $d_{I2\cdots Cl1}$ = 3.216(2) Å; $\angle_{C-I\cdots Cl}$ = 166.7(1)°, $\angle_{C-I\cdots Cl}$ = 170.5(1)°.

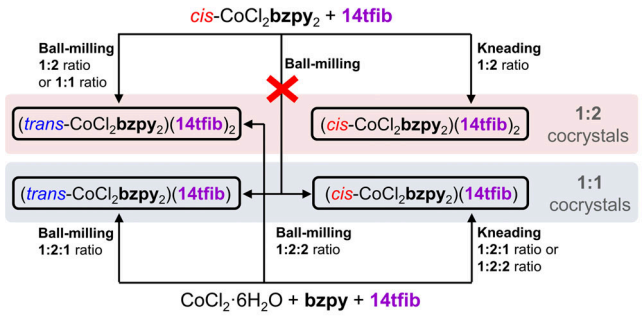

Scheme 1. Outcomes of mechanochemical synthesis of the four cocrystals involving $CoCl_2$**Bzpy**$_2$ and **14tfib**.

solid reactants and products of mechanochemical screening were characterized by PXRD, differential scanning calorimetry (DSC), and thermogravimetric analysis (TGA). An overview of mechanochemical transformations observed by LAG and kneading is shown in Scheme 1.

Attempts to synthesize the (*cis*-$CoCl_2$**bzpy**$_2$)(**14tfib**)$_2$ cocrystal by 30 min LAG of pre-synthesized solid *cis*-$CoCl_2$**bzpy**$_2$ and **14tfib** in the respective 1:2 stoichiometric ratio (see Supporting Information) unexpectedly gave the cocrystal of the corresponding *trans*-isomer (*trans*-$CoCl_2$**bzpy**$_2$)(**14tfib**)$_2$, as evidenced by comparison of the PXRD patterns measured for the milled material and calculated for the herein determined crystal structure.[41] The pure solid (*cis*-$CoCl_2$**bzpy**$_2$)(**14tfib**)$_2$ could not be obtained by ball-milling, even upon reducing the milling time, frequency, changing the milling assembly (the balls and the jar) from stainless steel to Teflon-covered,[42] or seeding the reaction mixture with pre-synthesized (*cis*-$CoCl_2$**bzpy**$_2$)(**14tfib**)$_2$ (see Supporting Information). To examine whether this outcome could be related to the *cis*→*trans* isomerization of the reagent *cis*-$CoCl_2$**bzpy**$_2$ upon mechanical treatment, the pure solid metal complex was ball-milled for 1 hour either neat, or in the presence of a small amount of EtOH. Analysis of the ball-milled material by PXRD in both cases revealed no sign of isomerization (see Supporting Information), indicating that *cis*-$CoCl_2$**bzpy**$_2$ alone does not undergo *cis*→*trans* isomerization by LAG, but requires the presence of **14tfib**. Switching to kneading, however, enabled the synthesis of (*cis*-$CoCl_2$**bzpy**$_2$)(**14tfib**)$_2$, indicating that the intensity of mechanical action also plays a role in the *cis*→*trans* isomerization that happens in the presence of **14tfib**.

Next, we explored the LAG reaction of equimolar amounts of *cis*-$CoCl_2$**bzpy**$_2$ and **14tfib** in a ball mill, in expectation to form the MOXB cocrystal containing the XB donors and acceptors in a 1:1 ratio, (*cis*-$CoCl_2$**bzpy**$_2$)(**14tfib**) (Figure 1). However, analysis of the reaction mixture after 30 min revealed the appearance of (*cis*-$CoCl_2$**bzpy**$_2$)(**14tfib**)$_2$, with longer milling yielding again (*trans*-$CoCl_2$**bzpy**$_2$)(**14tfib**)$_2$, in each case along with residual *cis*-$CoCl_2$**bzpy**$_2$.

To further understand the unexpected *cis*→*trans* isomerization of the *cis*-$CoCl_2$**bzpy**$_2$ moiety upon ball-milling in

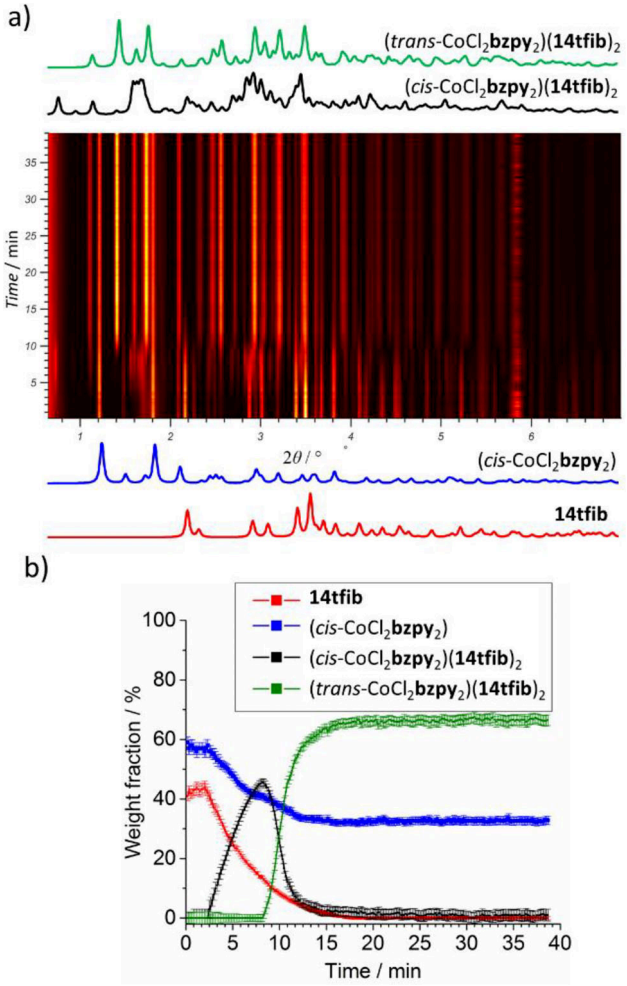

Figure 2. Results of in situ synchrotron PXRD ($\lambda = 0.20\,709$ Å) monitoring of the reaction of equimolar amounts of *cis*-$CoCl_2$**bzpy**$_2$ and **14tfib**: a) the time-resolved 2D PXRD plot, b) results of quantitative Rietveld analysis of the in situ obtained data.

the presence of **14tfib**, the mechanochemical reaction was monitored by in situ synchrotron PXRD at the Powder Diffraction and Total Scattering beamline P02.1 of the Deutsches Elektronen-Synchrotron (DESY). For these real-time monitoring experiments, the multicomponent reaction mixtures (300 mg of reactants solids, in the presence of 10 μL or 20 μL EtOH) were placed into X-ray transparent poly(methyl methacrylate) (PMMA) jars, along with two stainless steel balls (7 mm diameter, ca. 1.39 grams each), and the mixtures were milled on a modified Retsch MM400 vibration mill operating at 25 Hz (see Supporting Information). The monitoring experiments were performed on the mechanochemical reactions of *cis*-$CoCl_2$**bzpy**$_2$ and **14tfib** in respective 1:1 and 1:2 stoichiometric ratios, and sequential Rietveld refinement was performed for each in situ experiment. Analysis of the in situ monitoring data for the mechanochemical reaction of 1:1 amounts of *cis*-$CoCl_2$**bzpy**$_2$ and **14tfib** (Figure 2) revealed the appearance of the elusive (*cis*-$CoCl_2$**bzpy**$_2$)(**14tfib**)$_2$ after ca. 3 min milling, reaching a maximum content of ca. 45% by weight after ca. 8.5 min. The initially formed

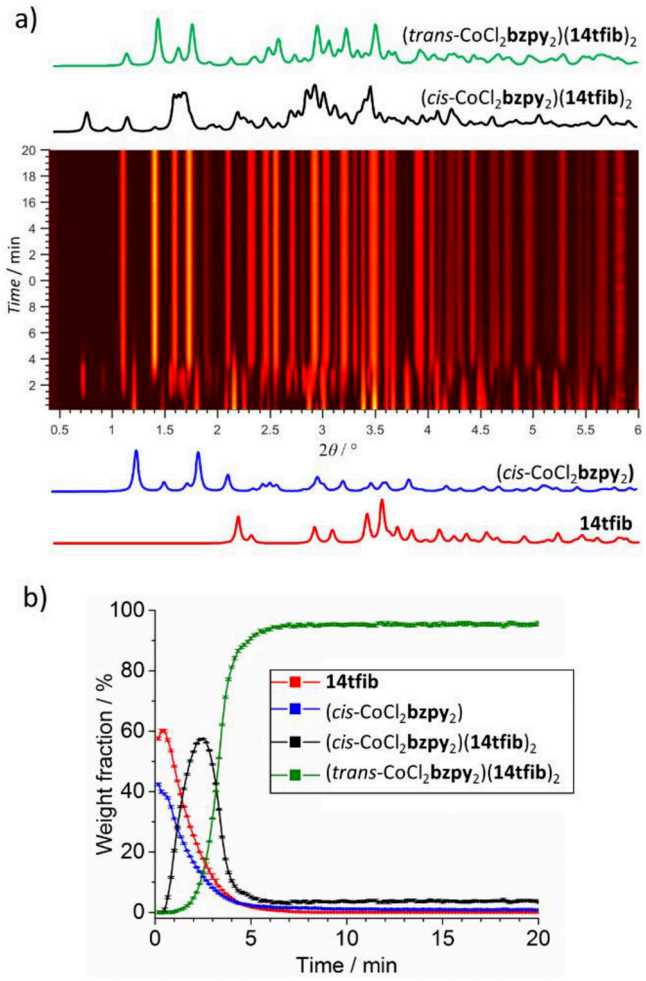

Figure 3. Results of in situ synchrotron PXRD ($\lambda = 0.20\,709$ Å) monitoring of the reaction of *cis*-$CoCl_2$**bzpy**$_2$ and **14tfib** in respective stoichiometric ratio 1:2: a) the time-resolved 2D PXRD plot, b) results of quantitative Rietveld analysis of the in situ obtained data.

(*cis*-$CoCl_2$**bzpy**$_2$)(**14tfib**)$_2$ is subsequently replaced by (*trans*-$CoCl_2$**bzpy**$_2$)(**14tfib**)$_2$. Notably, the in situ analysis shows that crystalline (*cis*-$CoCl_2$**bzpy**$_2$)(**14tfib**)$_2$ almost completely disappears after ca. 15 min, at which point the amount of (*trans*-$CoCl_2$**bzpy**$_2$)(**14tfib**)$_2$ remains constant. At the same time, the amount of residual solid *cis*-$CoCl_2$**bzpy**$_2$ also remains constant after the disappearance of (*cis*-$CoCl_2$**bzpy**$_2$)(**14tfib**)$_2$, indicating that the mechanochemical *cis*→*trans* isomerization of the metal complex involves the transient formation of the MOXB cocrystal.

Similar behaviour was observed for the mechanochemical reaction of *cis*-$CoCl_2$**bzpy**$_2$ and **14tfib** in the respective 1:2 stoichiometric ratio (Figure 3). Real-time monitoring revealed the rapid formation of (*cis*-$CoCl_2$**bzpy**$_2$)(**14tfib**)$_2$, with negligible amounts of residual *cis*-$CoCl_2$**bzpy**$_2$, reaching a maximum abundancy of ca. 56% by weight after ~2.5 min milling. The subsequent transformation into (*trans*-$CoCl_2$**bzpy**$_2$)(**14tfib**)$_2$ reached completion within ca. 7 min milling.

Overall, the outcomes of real-time and in situ monitoring of mechanochemical cocrystallization of *cis*-$CoCl_2$**bzpy**$_2$ and **14tfib** indicate that, whereas the *cis*-based MOXB cocrystal readily forms early in the reaction, upon milling it is replaced by the MOXB cocrystal of the corresponding *trans*-isomer of the metal-organic unit. Importantly, any residual *cis*-$CoCl_2$**bzpy**$_2$ that does not form the MOXB cocrystal does not undergo isomerization upon continued milling, as evidenced by in situ, as well as *ex situ* analyses.

The so far outlined mechanochemical procedures gave rise to either (*cis*-$CoCl_2$**bzpy**$_2$)(**14tfib**)$_2$ or (*trans*-$CoCl_2$**bzpy**$_2$)(**14tfib**)$_2$. In contrast, solution one-pot reactions of $CoCl_2{\cdot}6H_2O$, **bzpy** and **14tfib** have been observed to produce also the cocrystal containing the XB donor and acceptor in 1:1 stoichiometric ratio, (*cis*-$CoCl_2$**bzpy**$_2$)(**14tfib**). Consequently, the mechanochemical synthesis of (*cis*-$CoCl_2$**bzpy**$_2$)(**14tfib**) was attempted using the multi-component one-pot approach. Ball-milling of $CoCl_2{\cdot}6H_2O$, **bzpy** and **14tfib** in the respective 1:2:1 stoichiometric ratio along with small amount of EtOH gave after 30 min a new crystalline phase, whose PXRD pattern did not match to any of the starting materials, or the MOXBs obtained from solution. Crystal structure analysis from PXRD data revealed that the new phase is the MOXB cocrystal (*trans*-$CoCl_2$**bzpy**$_2$)(**14tfib**). The corresponding *cis*-cocrystal, (*cis*-$CoCl_2$**bzpy**$_2$)(**14tfib**), was subsequently obtained by kneading of the starting materials in the presence of EtOH (Scheme 1). Next, the one-pot multi-component reactions were explored using $CoCl_2{\cdot}6H_2O$, **bzpy** and **14tfib** in the respective 1:2:2 stoichiometric ratio. The LAG reaction in presence of EtOH yielded (*trans*-$CoCl_2$**bzpy**$_2$)(**14tfib**)$_2$, while kneading gave again the cocrystal (*cis*-$CoCl_2$**bzpy**$_2$)(**14tfib**) along with excess of **14tfib**. Overall, these experiments indicate that the herein employed ball-milling conditions facilitate the *cis*→*trans* isomerization, leading to the MOXB cocrystal with the *trans*-$CoCl_2$**bzpy**$_2$ core, while kneading enables the cocrystallization with the retention of the *cis*-isomer structure.

In order to explore whether the isomerization of the *cis*-$CoCl_2$**bzpy**$_2$ unit in the corresponding MOXB cocrystal could be only thermally-driven, the complex, and all herein prepared cocrystals, were also explored by simultaneous thermogravimetric analysis and differential scanning calorimetry (TGA/DSC). Thermal analysis of solid *cis*-$CoCl_2$**bzpy**$_2$ revealed a sharp endothermic signal with onset around 183 °C, simultaneous with a mass loss, indicating decomposition. The thermograms of the (*cis*-$CoCl_2$**bzpy**$_2$)(**14tfib**)$_2$ and the (*trans*-$CoCl_2$**bzpy**$_2$)(**14tfib**)$_2$ cocrystals were mutually similar, exhibiting a sharp endothermic signal with an onset around 147 and 137 °C, respectively, in both cases simultaneous with a weight change consistent with the loss of two molecules of **14tfib**. The cocrystals (*cis*-$CoCl_2$**bzpy**$_2$)(**14tfib**) and (*trans*-$CoCl_2$**bzpy**$_2$)(**14tfib**) also exhibited similar thermal signatures, with a sharp endothermic signal around 149 and 150 °C, respectively, in both cases associated with a change in weight indicative of the loss of one equivalent of **14tfib**. Overall, these experiments suggest that none of the MOXB cocrystals, or the solid *cis*-$CoCl_2$**bzpy**$_2$ undergo isomerization before thermal decomposition at high temperatures. Therefore, the observed conversion of (*cis*-$CoCl_2$**bzpy**$_2$)(**14tfib**)$_2$ into (*trans*-$CoCl_2$**bzpy**$_2$)(**14tfib**)$_2$ appears to be the result of the mechanical LAG treatment.

Table 1: Calculated $\Delta_r H$ values (in kJ mol^{-1}, per mol of product) for the herein explored reactions of formation and interconversion of MOXB cocrystals based on *cis*- and *trans*-forms of the metal-organic unit.

Reaction	$\Delta_r H$/kJ mol^{-1}
cis-$CoCl_2$**bzpy**$_2$ + 2 **14tfib** → (*cis*-$CoCl_2$**bzpy**$_2$)(**14tfib**)$_2$	−9.33
cis-$CoCl_2$**bzpy**$_2$ + 2 **14tfib** → (*trans*-$CoCl_2$**bzpy**$_2$)(**14tfib**)$_2$	−90.07
(*cis*-$CoCl_2$**bzpy**$_2$)(**14tfib**)$_2$ → (*trans*-$CoCl_2$**bzpy**$_2$)(**14tfib**)$_2$	−80.74
cis-$CoCl_2$**bzpy**$_2$ + **14tfib** → (*cis*-$CoCl_2$**bzpy**$_2$)(**14tfib**)	−3.36
(*cis*-$CoCl_2$**bzpy**$_2$)(**14tfib**) → (*trans*-$CoCl_2$**bzpy**$_2$)(**14tfib**)	−70.08

Finally, the reactions leading to the formation of herein reported MOXB cocrystals and their interconversion were also explored through periodic and molecular density-functional theory (DFT) calculations. The molecular DFT modelling for isolated *cis*- and *trans*-$CoCl_2$**bzpy**$_2$ molecules, performed in Gaussian 16 at PBE/6–311G(d,p)[43,44] level of theory, revealed that for a high-spin state the *cis*-isomer should be 8.2 kJ mol^{-1} enthalpically more favorable, whereas for a low-spin state the *trans*-isomer would be preferred by 12.7 kJ mol^{-1}. The preference for the formation of the *trans*-geometry metal complex is, however, greatly enhanced by cocrystallization: plane-wave periodic DFT calculations in CASTEP,[45] performed with PBE functional combined with many-body dispersion (MBD*)[46–48] correction scheme (Table 1), indicated that for the herein observed MOXB cocrystals the *trans*-isomers should be enthalpically preferred by 70–90 kJ mol^{-1}.[31–33] This result is consistent with observed LAG transformation of (*cis*-$CoCl_2$**bzpy**$_2$)(**14tfib**)$_2$ into (*trans*-$CoCl_2$**bzpy**$_2$)(**14tfib**)$_2$, which should be enthalpically favoured by ca. 81 kJ mol^{-1}.

The results of periodic DFT calculations indicate that the formation of the MOXB cocrystal provides an enhanced enthalpic driving force for the herein observed *cis*→*trans* isomerization of $CoCl_2$**bzpy**$_2$. A detailed mechanism for this process, however, remains unclear. Tentatively, we suggest that the formation of a halogen bond directly to one of the ligand atoms of the metal complex should weaken the associated coordination bond, overall making the coordination complex more labile, facilitating isomerization to *trans*-$CoCl_2$**bzpy**$_2$ that then leads to the thermodynamically more stable cocrystal. In such a scenario, MOXB cocrystal formation provides the thermodynamic driving force for *cis*→*trans* isomerization, with the formation of individual halogen bonds also making the metal complex sufficiently labile for such a process.

In summary, we have reported that halogen-bonded cocrystallization enables ball-milling isomerization of a *cis*-geometry coordination complex which is otherwise persistent in the solid state. Specifically, whereas solution-phase synthesis of herein explored $CoCl_2$**bzpy**$_2$ complex consistently yields the *cis*-isomer only, which does not undergo isomerization upon ball-milling neat or in the presence of a liquid, the formation of a halogen-bonded metal-organic (MOXB) cocrystal either from a metal salt or the pre-synthesized *cis*-$CoCl_2$**bzpy**$_2$ readily leads to *cis*-*trans* isomerization to form the corresponding *trans*-isomer as a halogen-bonded cocrystal. The observed *cis*→*trans* isomerization is also enthalpically-favored, with the *trans*-MOXB cocrystal being ca. 70–80 kJ mol^{-1} more exothermic compared to the *cis*-analogue. The necessity of forming a halogen-bonded cocrystal prior to ball-milling isomerization, as well as the persistence of pure solid *cis*-complex to such isomerization, are supported by real-time in situ PXRD monitoring of the process, which reveals the initial formation of a halogen-bonded cocrystal of the *cis*-complex which is rapidly replaced with the cocrystal of the *trans*-isomer, whereas any excess solid *cis*-complex persists throughout the milling experiment. In the context of mechanochemistry, these observations suggest a role for MOXB cocrystals as intermediates in otherwise not accessible mechanochemical transformations of coordination complexes, creating a link to cocrystal-mediated covalent bonds transformations seen in organic mechanosynthesis.[49–51] In the broader context of materials and supramolecular chemistry, these results provide a proof-of-principle for halogen bond-driven cocrystal formation as a means to modify reactivity of metal complexes, and present MOXB cocrystals as a class of materials that can exhibit new, responsive behaviours different from those of parent coordination compounds. Further mechanistic studies, as well as systematic exploration of such behavior in other MOXB cocrystal systems, based on diverse metal-organic complexes and halogen bond donors, are underway.

Supporting Information

The authors have cited additional references within the Supporting Information.[52–61] Deposition Number(s) 2081192 (for (*trans*-$CoCl_2$**bzpy**$_2$)(**14tfib**)), 2279597 (for (*trans*-$CoCl_2$**bzpy**$_2$)(**14tfib**)$_2$), 2279598 (for (*cis*-$CoCl_2$**bzpy**$_2$)(**14tfib**)), 2279599 (for (*cis*-$CoCl_2$**bzpy**$_2$)(**14tfib**)$_2$), and 2279600 (for *cis*-$CoCl_2$**bzpy**$_2$) contain(s) the supplementary crystallographic data for this paper. These data are provided free of charge by the joint Cambridge Crystallographic Data Centre and Fachinformationszentrum Karlsruhe Structures service.

Acknowledgements

This research was supported by the Croatian Science Foundation under the project IP-2014–09–7367 and project IP-2019–04–1868. The authors acknowledge the support of project CIuK co-financed by the Croatian Government and the European Union through the European Regional Development Fund-Competitiveness and Cohesion Operational Programme (Grant KK.01.1.1.02.0016.). MA would like to thank the National Science Center of Poland (NCN) for the financial support via the grant 2020/37/B/ ST5/02638. MA would also like to thank PLGrid for access to the Prometheus supercomputer, on which all the periodic DFT calculations were performed. TF acknowledges the support of the Leverhulme Trust (Leverhulme International Professorship), the University Of Birmingham, United Kingdom, and McGill University, Canada. The authors acknowledge DESY (Hamburg, Germany), a member of the Helmholtz Association HGF, for the provision of experimental facilities.

Parts of this research were carried out at PETRA III beamline P02.1. Beamtime was allocated by an In-House contingent.

Conflict of Interests

The authors declare no conflict of interest.

Data Availability Statement

The data that support the findings of this study are available in the Supporting Information of this article.

Keywords: Cocrystal · Halogen bond · Isomerization · Mechanochemistry · Metal

[1] W. Jones, W. D. S. Motherwell, A. V. Trask, *MRS Bull.* **2006**, *31*, 875–879.
[2] S. Karki, T. Friščić, L. Fábián, P. R. Laity, G. M. Day, W. Jones, *Adv. Mater.* **2009**, *21*, 3905–3909.
[3] T. Friščić, W. Jones, *J. Pharm. Pharmacol.* **2010**, *62*, 1547–1559.
[4] B. Sandhu, A. S. Sinha, J. Desper, C. B. Aakeröy, *Chem. Commun.* **2018**, *54*, 4657–4660.
[5] O. Shemchuk, S. d'Agostino, C. Fiore, V. Sambri, S. Zannoli, F. Grepioni, D. Braga, *Cryst. Growth Des.* **2020**, *20*, 6796–6803.
[6] I. Brekalo, V. Martinez, B. Karadeniz, P. Orešković, D. Drapanauskaite, H. Vriesema, R. Stenekes, M. Etter, I. Dejanović, J. Baltrusaitis, K. Užarević, *ACS Sustainable Chem. Eng.* **2022**, *10*, 6743–6754.
[7] O. S. Bushuyev, T. C. Corkery, C. J. Barrett, T. Friščić, *Chem. Sci.* **2014**, *5*, 3158–3164.
[8] J. Vainauskas, F. Topić, O. S. Bushuyev, C. J. Barrett, T. Friščić, *Chem. Commun.* **2020**, *56*, 15145–15148.
[9] A. A. Dar, S. Rashid, *CrystEngComm* **2021**, *23*, 8007–8026.
[10] O. Bolton, A. J. Matzger, *Angew. Chem. Int. Ed.* **2011**, *50*, 8960–8963.
[11] H. M. Titi, M. Arhangelskis, G. P. Rachiero, T. Friščić, R. D. Rogers, *Angew.Chem.* **2019**, *131*, 18570.
[12] J. Zhang, J. M. Shreeve, *CrystEngComm* **2016**, *18*, 6124–6133.
[13] G. Cavallo, P. Metrangolo, R. Milani, T. Pilati, A. Priimagi, G. Resnati, G. Terraneo, *Chem. Rev.* **2016**, *116*, 2478–2601.
[14] *Halogen Bonding, Fundamentals and Applications*, (Eds. P. Metrangolo, G. Resnati), Springer-Verlag, Berlin, Heidelberg, **2008**.
[15] C. R. Groom, I. J. Bruno, M. P. Lightfoot, S. C. Ward, *Acta. Cryst.* **2016**, *B72*, 171.
[16] M. Fourmigué, *Curr. Opin. Solid State Mater. Sci.* **2009**, *13*, 36–45.
[17] R. W. Troff, T. Mäkelä, F. Topić, A. Valkonen, K. Raatikainen, K. Rissanen, *Eur. J. Org. Chem.* **2013**, *2013*, 1617–1637.
[18] R. Bertani, P. Sgarbossa, A. Venzo, F. Lelj, M. Amati, G. Resnati, T. Pilati, P. Metrangolo, G. Terraneo, *Coord. Chem. Rev.* **2010**, *254*, 677–695
[19] V. Nemec, K. Lisac, N. Bedeković, L. Fotović, V. Stilinović, D. Cinčić, *CrystEngComm* **2021**, *23*, 3063–3083.
[20] D. M. Kryukov, A. A. Khrustaleva, S. V. Baykov, R. M. Gomila, A. Frontera, V. Yu. Kukushkin, A. V. Rozhkov, N. A. Bokach, *Inorg. Chem. Commun.* **2025**, *182*, 115288.
[21] A. V. Rozhkov, I. V. Ananyev, A. A. Petrov, B. Galmés, A. Frontera, N. A. Bokach, V. Yu. Kukushkin, *Cryst. Growth. Des.* **2021**, *21*, 4073–4082.
[22] H. Hachem, O. Jeannin, M. Fourmigué, F. Barrière, D. Lorcy, *CrystEngComm* **2020**, *22*, 3579–3587.
[23] M. C. Pfrunder, J. J. Whittaker, S. Parsons, B. Moubaraki, K. S. Murray, S. A. Moggach, N. Sharma, A. S. Micallef, J. K. Clegg, J. C. McMurtrie, *Chem. Mater.* **2020**, *32*, 3229–3234.
[24] J.-C. Christopherson, K. P. Potts, O. S. Bushuyev, F. Topić, I. Huskić, K. Rissanen, C. J. Barrett, T. Friščić, *Faraday Discuss.* **2017**, *203*, 441.
[25] K. Lisac, D. Cinčić, *Cryst. Eng. Comm.* **2018**, *20*, 5955–5963.
[26] K. Lisac, D. Cinčić, *Crystals* **2017**, *7*, 363.
[27] K. Lisac, S. Cepić, M. Herak, D. Cinčić, *Chem. Methods.* **2022**, *2*, e202100088.
[28] V. Nemec, R. Sušanj, N. Baus Topić, D. Cinčić, *Chem. Asian J.* **2025**, *20*, e202401916.
[29] M. A. Sinnwell, L. R. MacGillivray, *Angew. Chem. Int. Ed.* **2016**, *55*, 3477–3480.
[30] V. K. Seiler, N. Tumanov, K. Robeyns, B. Champagne, J. Wouters, T. Leyssens, *Cryst. Growth. Des.* **2020**, *20*, 608.
[31] L. Kumar, K. Leko, V. Nemec, D. Trzybiński, N. Bregović, D. Cinčić, M. Arhangelskis, *Chem. Sci.* **2023**, *14*, 3140–3146.
[32] M. Arhangelskis, F. Topić, P. Hindle, R. Tran, A. J. Morris, D. Cinčić, T. Friščić, *Chem. Commun.* **2020**, *56*, 8293–8296.
[33] K. Lisac, F. Topić, M. Arhangelskis, S. Cepić, P. A. Julien, C. W. Nickels, A. J. Morris, T. Friščić, D. Cinčić, *Nat. Commun.* **2019**, *10*, 61.
[34] S. L. James, C. J. Adams, C. Bolm, D. Braga, P. Collier, T. Friščić, F. Grepioni, K. D. M. Harris, G. Hyett, W. Jones, A. Krebs, J. Mack, L. Maini, A. G. Orpen, I. P. Parkin, W. C. Shearouse, J. W. Steed, D. C. Waddell, *Chem. Soc. Rev.* **2012**, *41*, 413–447.
[35] T. Friščić, C. Mottillo, H. M. Titi, *Angew. Chemie – Int. Ed.* **2020**, *59*, 1018.
[36] J. Andersen, J. Mack, *Green Chem.* **2018**, *20*, 1435–1443.
[37] T. Friščić, S. L. Childs, S. A. A. Rizvi, W. Jones, *CrystEngComm* **2009**, *11*, 418–426.
[38] T. Friščić, W. Jones, *Growth Des.* **2009**, *9*, 1621–1637.
[39] D. Braga, F. Grepioni, *Angew. Chem. Int. Ed.* **2004**, *43*, 4002–4011.
[40] D. Braga, L. Maini, F. Grepioni, *Chem. Soc. Rev.* **2013**, *42*, 7638.
[41] On two occasions, however, the LAG synthesis produced the (*cis*-$CoCl_2$**bzpy**$_2$)(**14tfib**)$_2$ cocrystal. The origin of this result is unclear, as even subsequent attempts to seed the ball-milling reaction with (*cis*-$CoCl_2$**bzpy**$_2$)(**14tfib**)$_2$ yielded the cocrystal of the trans-isomer.
[42] K. S. McKissic, J. T. Caruso, R. G. Blair, J. Mack, *Green Chem.* **2014**, *16*, 1628.
[43] *Gaussian 16*, Revision B.01, M. J. Frisch, G. W. Trucks, H. B. Schlegel, G. E. Scuseria, M. A. Robb, J. R. Cheeseman, G. Scalmani, V. Barone, G. A. Petersson, H. Nakatsuji, X. Li, M. Caricato, A. V. Marenich, J. Bloino, B. G. Janesko, R. Gomperts, B. Mennucci, H. P. Hratchian, J. V. Ortiz, A. F. Izmaylov, J. L. Sonnenberg, D. Williams-Young, F. Ding, F. Lipparini, F. Egidi, J. Goings, B. Peng, A. Petrone, T. Henderson, D. Ranasinghe, et al., Gaussian, Inc., Wallingford CT, **2016**.
[44] J. P. Perdew, K. Burke, M. Ernzerhof, *Phys. Rev. Lett.* **1996**, *77*, 3865–3868.
[45] S. J. Clark, M. D. Segall, C. J. Pickard, P. J. Hasnip, M. I. J. Probert, K. Refson, M. C. Payne, *Z. Kristallogr.* **2005**, *220*, 567–570.
[46] A. Tkatchenko, R. A. DiStasio, R. Car, M. Scheffler, *Phys. Rev. Lett.* **2012**, *108*, 236402.
[47] A. Ambrosetti, A. M. Reilly, R. A. DiStasio, A. Tkatchenko, *J. Chem. Phys.* **2014**, *140*, 18A508.
[48] A. M. Reilly, A. Tkatchenko, *Chem. Sci.* **2015**, *6*, 3289–3301.
[49] K. J. Ardila-Fierro, J. G. Hernández, *Angew. Chem. Int. Ed.* **2024**, *63*, e202317638.

[50] S. Lukin, M. Tireli, I. Lončarić, D. Barišić, P. Šket, D. Vrsaljko, M. Di Michiel, J. Plavec, K. Užarević, I. Halasz, *Chem. Commun.* **2018**, *54*, 13216–13219.
[51] A. N. Sokolov, D.-K. Bučar, J. Baltrusaitis, S. X. Gu, L. R. MacGillivray, *Angew. Chem. Int. Ed.* **2010**, *49*, 4273–4277.
[52] T. Degen, M. Sadki, E. Bron, U. König, G. Nénert, *Powder Diffr.* **2014**, *29*, S13–S18.
[53] *CrysAlis CCD V171.Vol. 34, Oxford Diffraction*, **2003**, Oxford Diffraction Ltd., Abingdon, Oxfordshire, UK.
[54] *CrysAlis RED V171.Vol. 34, Oxford Diffraction*, **2003**, Oxford Diffraction Ltd., Abingdon, Oxfordshire, UK.
[55] G. M. Sheldrick, *Acta Crystallogr.* **2015**, *A71*, 3.
[56] G. M. Sheldrick, *Acta Crystallogr.* **2008**, *A64*, 112–122.
[57] L. J. Farrugia, *J. Appl. Crystallogr.* **1999**, *32*, 837–838.
[58] C. F. Macrae, I. J. Bruno, J. A. Chisholm, P. R. Edgington, P. McCabe, E. Pidcock, L. Rodriguez-Monge, R. Taylor, J. Van De Streek, P. A. Wood, *J. Appl. Crystallogr.* **2008**, *41*, 466.
[59] Bruker AXS, TOPAS, Version 5, Bruker AXS, Karlsruhe, Germany, **2014**.
[60] Mettler-Toledo GmbH, STARe Software, Version 15.00, Mettler-Toledo GmbH, Schwerzenbach, Switzerland, **2016**.
[61] T. Björkman, *Comput. Phys. Commun.* **2011**, *182*, 1183–1186.

Manuscript received: August 03, 2025
Revised manuscript received: September 01, 2025
Manuscript accepted: September 19, 2025
Version of record online: October 06, 2025